Microfluidic logic gates and timers†

Michael W. Toepke, Vinay V. Abhyankar and David J. Beebe*

Received 11th June 2007, Accepted 30th July 2007
First published as an Advance Article on the web 7th September 2007
DOI: 10.1039/b708764k

We use surface tension-based passive pumping and fluidic resistance to create a number of microfluidic analogs to electronic circuit components. Three classes of components are demonstrated: (1) OR/AND, NOR/NAND, and XNOR digital microfluidic logic gates; (2) programmable, autonomous timers; and (3) slow, perfusive flow rheostats. The components can be implemented with standard pipettes and provide a means of non-electronic and autonomous preprogrammed control with potential utility in cell studies and high throughput screening applications.

Introduction

Microfluidic devices have been used to explore a variety of biological problems of interest, ranging from fundamental research in protein crystallization[1] to diagnostic assays.[2] A number of these applications require the integration of valves, mixers, and other components into the devices in order to successfully carry out various steps. The incorporation of actively controlled functionalities, either directly in the device or *via* a fixed interface with external components, often leads to more complex fabrication and the need for ancillary equipment. The use of passive and autonomous microfluidic components, while sometimes requiring more complex fabrication, can help to reduce or eliminate the need for additional equipment. Eliminating external components makes point-of-care devices more portable and facilitates operation of many devices in parallel, which is of particular interest for large parametric screening applications. In this paper, we demonstrate three new classes of microfluidic components based on passive pumping that are analogous to electronic circuit components.

Many of the fabrication methods used to create microfluidic devices were first developed for microelectronics, so it is fitting that a number of parallels can be drawn between the two fields. Resistance, driving forces (pressure/voltage), and current (fluid/electrons) analogies are commonly used to compare electronic components and fluid networks. The analogy has been further extended in microfluidics to include diodes, rectifiers,[3] memory elements,[4] and capacitors. Two-phase flow has recently been used to encode and decode data sets using droplets.[5] As with electronics, microfluidic components can be combined to form more complex devices, and a microfluidic breadboard has already been demonstrated.[6] Microfluidics can also be used to address problems that are not easily solved using standard computational methods.[7]

Regulatory systems can also be implemented in microfluidic devices. Responsive hydrogels have been used in microfluidic devices to regulate the pH[8] or temperature of a solution.[9] The use of pneumatic control in 3D channel structures has been shown as a means of self-regulating flow.[10] Coupling a conditional action to more than one input enables the creation of logic gates, which can be combined to perform computation and more complex functions.

Logic gates

Fluidic logic elements can be traced back to the 1950s; however, most of the early constructs depended on turbulent and multi-stable flow states,[11] which are not scalable due to the low Reynolds numbers that are typically observed in microfluidic channels. More recent efforts using microfluidics have employed fluidic resistance,[12] electrochemistry,[13] pneumatics,[14] channel geometry,[15] multiphase flow,[16] and chemistry[17] to create logic elements. Many of these approaches rely on continuous flow and are unable to create more integrated constructs due to different input/output (*e.g.* pressure/dye). Additionally, the electronic components used to input and read out signals are often more complex than the devices themselves. For many applications, it would be advantageous for fluidic logic elements to use consistent signal input/output and require minimal supporting equipment.

While liquid-based logic devices are not likely to compete with solid-state technologies in terms of computational power, they offer a facile method for implementing autonomous control in microfluidic systems. We have developed a new class of fluidic logic gates that use a consistent input/output (droplet/droplet), visual signal transduction (droplet/no droplet), and allows several gates to be connected in series. The method is based on a previously reported passive pumping technique that uses the pressure differential between surfaces with different radii of curvature.[18] Importantly, the method can be implemented *via* ubiquitous pipetting (either manual or automated).

In passive pumping, the radius of curvature can be thought of as a voltage in an electronic circuit. Flow within the circuit will be directed from high potential, or small radius of curvature, to regions of lower potential, *i.e.* a larger radius of curvature. Further, a digital input/output can be defined by

Department of Biomedical Engineering, University of Wisconsin Madison, WI, 53706, USA. E-mail: djbeebe@wisc.edu
† Electronic supplementary information (ESI) available: Movie files. See DOI: 10.1039/b708764k

using the presence of a droplet at a location to represent a value of 1 and the absence of a droplet to represent 0.

Using this construct, an inverter can be created using a microfluidic channel with two ports, as shown in Fig. 1. A droplet is placed on one of the ports, which serves as the output. If there is an input of 0, *i.e.* no droplet placed on the other port, the output is 1. If a larger droplet is placed on the inlet, the output droplet will be pumped away to give an output of 0. Similarly, a NOR gate can be constructed by adding a second input port to the inverter structure. An output of 1 is registered as long as both inputs are 0. However, if a droplet is placed on either or both of the input ports, a 0 readout will result. The operation of a NOR gate is shown in Fig. 1c and d.

OR/AND gates require an output of 1 only if at least one of the inputs is 1. In the present system, this would require liquid to be pumped to a port were there is originally no droplet. While a larger droplet has traditionally been used as a low-pressure sink in the passive pumping method, it is not a necessity. For the OR/AND gates, we create an output port with a radius larger than that of the input droplet. The curvature of the meniscus in the outlet port is large enough to drive fluid flow to the outlet from the inlet, provided a sufficiently small input droplet is used. The resulting fluid flow then displaces the air/liquid interface from within the port to above the port to form a droplet. A functional AND gate is shown in Fig. 1e–g and a movie of the operating gate can be seen in movie 1 of the ESI.† The same design can be used as an OR gate or an AND gate by simply changing the size or number of droplets that are used to define an input of 1, which implies that the passive pumping logic devices are to some extent programmable. That is to say, the size of the input and priming droplets can be varied to change the type of gate that is created with a given channel geometry.

A NAND gate can be constructed by arranging two channels near one another. The main channel contains three ports for the two inputs and the output. The output port is primed with a droplet prior to placing any input droplets and a second channel is placed in close proximity to the output droplet. If any input droplets are placed, they will increase the size of the output droplet. If only one input droplet is placed, the output droplet will grow in size but will not overlap with the inlets of the second channel. However, if there are droplets placed on both inputs, the output droplet will grow large enough to overlap with the inlet of the second channel. The output droplet will then be pumped away through the secondary channel, leaving an output of 0. The NAND gate can be operated as a NOR gate by increasing the size of the priming output droplet or the input droplet. A sequence of images showing a functioning NAND gate is shown in Fig. 2, which can also be seen as a video (movie 2, ESI†).

An XNOR gate can be formed by modifying the secondary channel of the NAND/NOR design to have a high fluidic resistance. The output of the XNOR gate is primed with a droplet, as with the NAND/NOR configuration. A single input droplet is sufficient to create fluid contact between the two channels and will lead to the droplet being pumped away, though at a slower rate than in the case of the NOR gate. The addition of a second input droplet can then be used to increase the output droplet volume such that it is larger than the sink, provided that the output droplet grows much faster than the sink droplet. Thus, the output droplet remains only if the inputs are 0/0 or 1/1. Fig. 3 shows the operation of the XNOR gate. The main channel is 250 μm tall while the secondary channel is only 40 μm tall, providing significantly higher fluidic resistance. The gate is set by placing a 1.2 μl droplet on the output port and a 2.5 μl droplet on the sink. Input droplets with a volume of 0.9 μl were used to operate the gate. The input ports to the secondary channel are shorter than on the

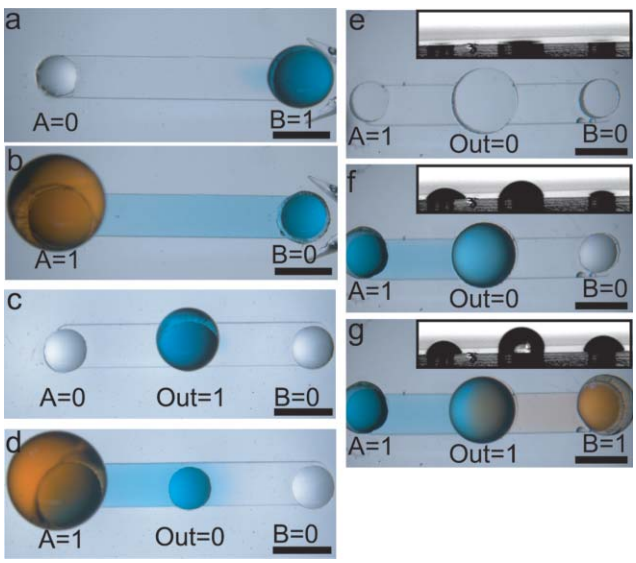

Fig. 1 Microfluidic inverter, AND, and NOR gates. The inverter consists of a single channel with two ports for input A and output B, shown for an input of (a) 0 and (b) 1. The NOR gate contains three ports for the inputs A and B and the output, shown for inputs of (c) 0/0 and (d) 1/0. The AND gate contains two smaller ports for inputs A and B and a larger port for the output, shown for inputs of (e) 0/0, (f) 1/0, and (g) 1/1. (Scalebar = 1 mm.)

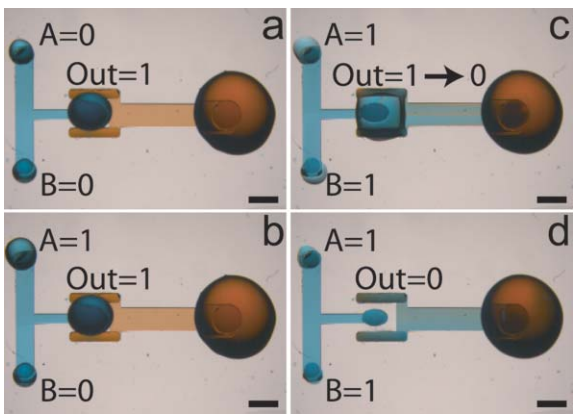

Fig. 2 Microfluidic NAND gate using two separate channels. The NAND gate consists of a main channel with two input ports and an output port, which is placed in close proximity to a secondary channel used to draw away the output droplet for inputs of 1/1. (a) Gate with 0/0 input and output of 1. (b) Gate with 1/0 input and output of 1. (c) Gate with 1/1 input transitioning from an output of 1 to 0. (d) Gate with 1/1 input with final output of 0. (Scalebar = 1 mm.)

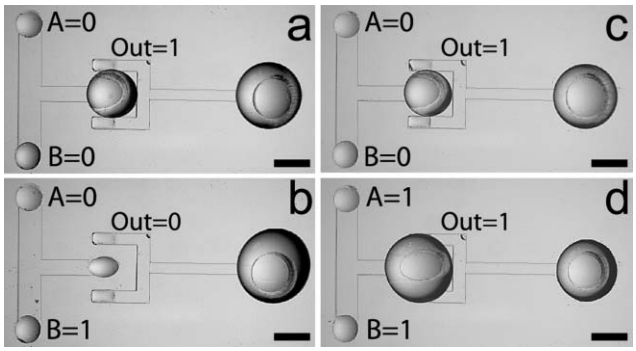

Fig. 3 Microfluidic XNOR gate using two channels. The XNOR gate consists of a main channel with input and output ports, along with a high resistance secondary channel to remove the output droplet when only one of the inputs has a value of 1. (a) Gate with 0/0 input and output of 1. (b) Gate with 1/0 input and output 0. (c) The same conditions as shown in (a). (d) Gate with inputs of 1/1 and output of 1. The droplet sizes for the input, initial output, and sink were 0.9, 1.2, and 2.5 μl. Channel edges are outlined for clarity. (Scalebar = 1 mm.)

NAND gate in order to maintain a droplet shape after the output overlaps with the secondary channel ports.

Multi-channel designs can also be used to merge and split individual droplets. Fig. 4 shows a three-channel design that

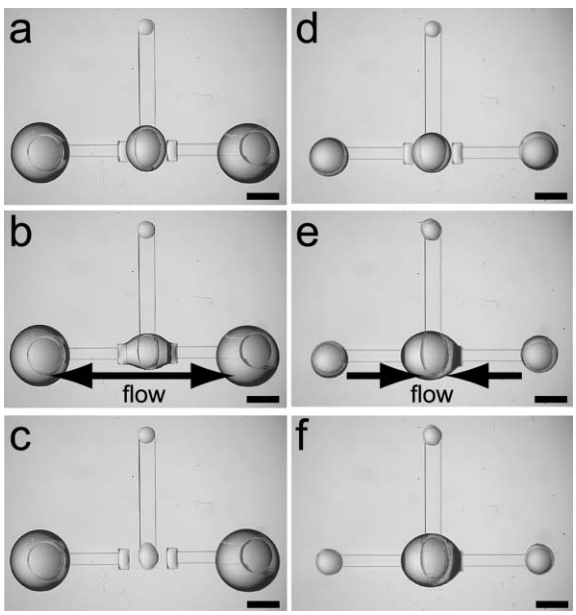

Fig. 4 Droplets can be split into separate volumes or merged with other droplets. (a) A three-channel structure is primed with a small droplet (1.1 μl) at the output port of the central channel and large droplets (2.4 μl) on the output ports of the two outer channels. (b) A 0.5 μl droplet is placed on the input of the central channel, temporarily increasing the volume of the central droplet so that it connects all three channels. (c) The central droplet is split between the two output droplets of the outer channels. (d) The three-channel structure is primed with droplets on the outlets of the central channel (0.95 μl) and the two outer channels (0.75 μl). (e) A 0.5 μl droplet is placed on the input of the central channel, increasing the output volume and connecting the channels. (f) The output droplets of the outer channels are merged with the output droplet of the central channel. Channel edges are outlined for clarity. (Scalebar = 1 mm.)

can be used to either split an individual droplet or merge two separate droplets. The output droplet of the central channel can be split between the two side channels if its curvature is smaller than both of the outer channels (Fig. 4a–c and movie 3, ESI†). Alternatively, the central droplet can be used to mix the two droplets from the outer channels if the curvature of the central droplet is larger than both the outer droplets (Fig 4d–f and movie 4, ESI†). A number of channels can be connected in series by using the output of a preceding channel as the input for next channel, as shown in Fig. 5 (movie 5, ESI†). In addition to potentially enabling several gates to be connected in series, the cascading nature of some of the gates confers a degree of temporal control over subsequent pumping steps. That is, a set amount of time is required for the initial input droplet(s) to be pumped through a given channel before the output droplet will reach a critical size to carry out the next pumping step.

Passive timer

Periodic medium exchange, transient treatments with exogenous factors, and immunostaining are just a few examples of routine cell biology experiments that require a sequence of pipetting steps over a period of time. Time-dependent treatments are often inconvenient because they require a physical presence to remove cells from an incubator, pipette, and replace the cells in the incubator. In addition to being inconvenient, removal of cells from an incubator for treatment steps is not desirable because it exposes the sample, and the rest of the incubator contents, to fluctuations in temperature and atmospheric composition. Such stresses can alter cell behavior, which could fundamentally alter experimental results. Frequent handling of samples also increases the chance of contamination. Ideally, all of the dispensing steps needed to carry out a given experiment could be done at one time so that cell culture samples only have to be removed from incubators for endpoint analysis.

A passive timer can be constructed with a two-channel design similar to the NAND gate. The timer channel is made with a high fluidic resistance channel that acts like an hourglass of sorts, with fluid moving from one end of the channel to the other. The exit of the timer channel is placed in close proximity to the entrance of the main channel that is to be treated after a given period of time. The outlet droplet of

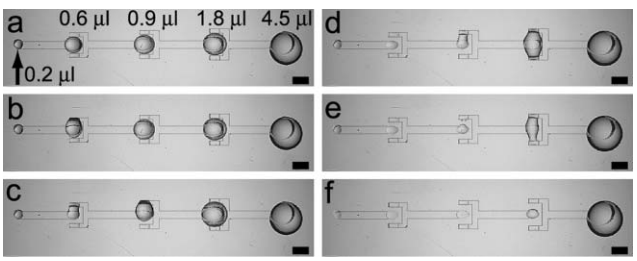

Fig. 5 A cascade of passive pumping steps. The volume of each successive droplet is larger than the sum of the proceeding droplets. (a) The channels primed just prior to adding a small droplet to set off the cascade. (b)–(f) A series of images after the cascade has been set off. Channel edges outlined for clarity. (Scalebar = 1 mm.)

the timing channel grows as fluid is pumped through the high-resistance channel and the droplet eventually grows large enough to overlap the inlet port, creating a connection between the two channels. If the pressure in the droplet connecting the two channels is greater than the pressure at the outlet of the main channel, the fluid connecting the two channels will be pumped through the main channel. The droplet connecting the two channels can be completely pumped away or a portion of the liquid can be left behind to maintain the connection, depending on the port design. The time required to achieve fluidic connection is determined by the resistance of the timer channel, *i.e.* the channel dimensions, and by the size of the inlet and outlet droplets. A representative timer can be seen in Fig. 6a–c. This design uses a curved input port for the main channel in order to maintain a connection between the two channels (movie 6, ESI†).

A channel with multiple inlets can be used to provide a variable fluidic resistance, allowing for a wide range of times to be set using a single device. Time delays ranging from a few seconds to a number of hours can be achieved by varying the channel resistance and initial pressure differential. Further, multiple timing channels can be used to carry out a series of treatments on an individual channel (movie 7, ESI†). Fig. 6d–f shows a device with two multi-port timer channels. The timer on the left was set for a longer time by placing an input droplet at the port furthest away from the sink droplet and the timer on the right was set for a short time by placing on the port nearest the main channel. Fig. 6d shows the device just after both of the ~0.65 μl input droplets have been placed, along with the 1.1 μl timer sink droplets and the 3.75 μl main channel sink. Fig. 6e shows the device just after the fluid from the short timer on the right has pumped through the main channel, which occurred after approximately eight seconds. Fig. 6f shows the device after the fluid in the timer on the left has been pumped through the main channel after just over one minute after the timer was set. Evaporation is of minor consequence for short timer settings, but can significantly alter outcomes for times longer than a few minutes if humidity control is not provided.

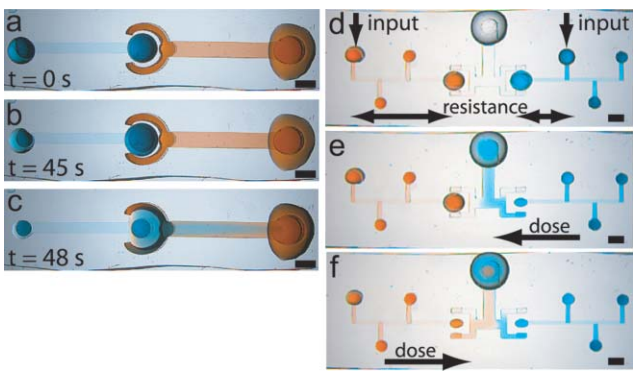

Fig. 6 Autonomous microfluidic timers based on passive pumping. The basic structure consists of a high resistance channel that provides slow flow to act as a timer and a second channel to pump the timer output droplet through once its volume has exceeded a critical size. (a) A single timer structure is shown with the high resistance timer channel on the left (blue) and the main channel is on the right (red), shown just after the input droplet was placed. (b) 45 seconds after placing the input droplet and (c) 48 seconds after placing the droplet, showing the outlet droplet of the timer flowing into the main channel. Multiple timer mechanisms can also be connected to a single microfluidic channel. (d) Input droplets of 0.65 μl are placed on ports of the two timers. The droplet on the left timer is placed on the outer most port, offering the highest resistance path. The droplet placed on the right timer is placed on the port nearest the output droplet, which is 1.1 μl in size, giving a lower resistance. (e) After 10 seconds, the output droplet of the timer on the right has pumped through the main channel while the timer on the left is still running. (f) The output droplet of the left timer has passively pumped through the main chamber after a minute. (Scalebar = 1 mm.)

Flow rheostat

The multi-inlet design used for the variable timer structure can also be used to generate continuous slow perfusion by connecting it directly to the main channel, as shown in Fig. 7. Flow rates as low as 100 nl per minute have been achieved with the system, with the lower limit being determined by the rate of evaporative flow that counters the surface tension-based pumping. The flow rate varies over the course of the pumping due to the changing volume of the source and sink droplets; however, the variation is gradual because the volumetric flow rate is small relative to the overall droplet size for a significant portion of the process.[18] A video of the slow flow device can be seen in movie 8 of the ESI.†

Transient flows can be observed when a small droplet is placed between two relatively larger droplets with different

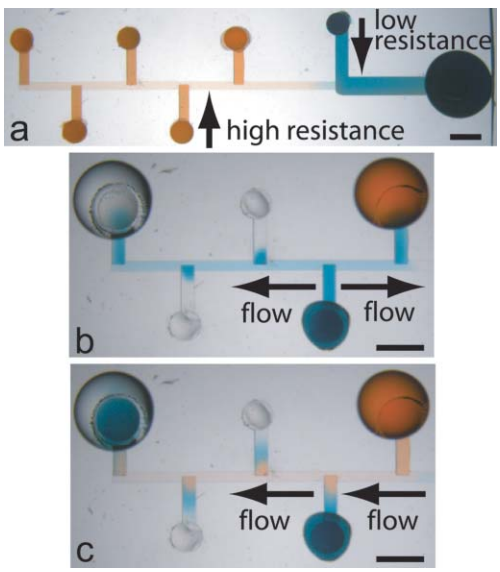

Fig. 7 Multi-port microfluidic channel for slow perfusion and transient flow. (a) The main channel (blue) is connected to a multi-port channel that has a high fluidic resistance (red). The multi-port, high resistance design serves as a rheostat to enable control over the flow rate in passive pumping. The multi-port design allows multiple input droplets to be placed, which can lead to transient flows. (b) A small droplet (0.5 μl) is placed between two larger droplets and pumps to both. The droplet to the left (colorless) has an initial volume of 3 μl and the droplet to the right has a volume of 2.5 μl. Pumping from the middle droplet eventually stops and flow goes from the droplet on the right to the droplet on the left. (Scalebar = 1 mm.)

volumes and resistance paths, as shown in Fig. 7b and c (movie 9, ESI.†). A 3 μl droplet is placed to the far right of the channel and a 2.5 μl droplet is placed to the far right. Very little flow is observed initially going from the right to the left because of the high fluidic resistance of the channel between the two droplets and the small relative volume difference between the two droplets. A 0.5 μl droplet is then placed between the two droplets, nearest to the droplet on the right. The high internal pressure of the small droplet is sufficient to drive flow towards both of the outer droplets. This flow essentially isolates the two samples with convective flow, acting as a mass transport valve. Eventually, flow from the smaller droplet stops and flow is initiated from the droplet on the right to the droplet on the left. Such an approach could also be used to achieve timed dosing of samples, provided reactive components are appropriately isolated.

Experimental

SU8 master molds were made using standard soft lithography procedures.[19] The devices were fabricated using polydimethylsiloxane (Sylgard 184, Dow Corning) at the prescribed 10 : 1 base to crosslinker ratio and cured using exclusion molding[20] on a hotplate at 72 °C for 2.5 hours. The PDMS replicas were then mounted on polystyrene substrates to complete the channel structure.

Conclusions

In conclusion, we have demonstrated a new method for implementing fluidic logic and temporal control in microfluidic devices using passive pumping. The method provides an easy way to integrate functionalities into microfluidic devices without adding complexity to the fabrication process and limits the dependence on external equipment. The method can be implemented in a high throughput manner with the use of ubiquitous multi-channel pipettes and robotic dispensers, facilitating use in cell biology research and screening applications. While the current designs use the active placement of droplets, platforms could also be constructed using responsive hydrogels to initiate fluid movement.[21] The input ports could be isolated from the output droplet by a hydrogel wall. If a certain condition is met in the solution, such as a pH or the presence of a specific biomolecule, the wall could shrink to fluidically connect the input to the output. Additionally, one can envision coupling the autonomous fluidic logic presented here with other autonomous components[22] to enable further integrated functionality.

Acknowledgements

We thank Keil Regehr and Jay Warrick for helpful discussions. This work was supported by funding from the Army Breast Cancer Research Program (W81XWH-04-1-0572), National Institutes of Health (K25 CA104162), and NHGRI training grant 5T32HG002760 (M.W.T.).

References

1 C. L. Hansen, E. Skordalakes, J. M. Berger and S. R. Quake, *Proc. Natl. Acad. Sci. U. S. A.*, 2002, **99**, 16531–16536; B. Zheng, L. S. Roach and R. F. Ismagilov, *J. Am. Chem. Soc.*, 2003, **125**, 11170–11171.
2 J. Moorthy, G. A. Mensing, D. Kim, S. Mohanty, D. T. Eddington, W. H. Tepp, E. A. Johnson and D. J. Beebe, *Electrophoresis*, 2004, **25**, 1705–1713; C. J. Easley, J. M. Karlinsey, J. M. Bienvenue, L. A. Legendre, M. G. Roper, S. H. Feldman, M. A. Hughes, E. L. Hewlett, T. J. Merkel, J. P. Ferrance and J. P. Landers, *Proc. Natl. Acad. Sci. U. S. A.*, 2006, **103**, 19272–19277; M. A. Burns, B. N. Johnson, S. N. Brahmasandra, K. Handique, J. R. Webster, M. Krishnan, T. Sammarco, P. M. Man, D. Jones, D. Heldsinger, C. H. Mastrangelo and D. T. Burke, *Science*, 1998, **282**, 484–487; R. H. Liu, M. J. Lodes, T. Nguyen, T. Siuda, M. Slota, H. S. Fuji and A. McShea, *Anal. Chem.*, 2006, **78**, 4184–4193; K. Sato and T. Kitamori, *J. Nanosci. Nanotechnol.*, 2004, **4**, 575–579.
3 A. Groisman and S. R. Quake, *Phys. Rev. Lett.*, 2004, **92**(094501), 094501–094501.
4 A. Groisman, M. Enzelberger and S. R. Quake, *Science*, 2003, **300**, 955–958.
5 M. J. Fuerstman, P. Garstecki and G. M. Whitesides, *Science*, 2007, **315**, 828–832.
6 K. A. Shaikh, K. S. Ryu, E. D. Goluch, J.-M. Nam, J. Liu, C. S. Thaxton, T. N. Chiesl, A. E. Barron, Y. Lu, C. A. Mirkin and C. Liu, *Proc. Natl. Acad. Sci. U. S. A.*, 2005, **102**, 9745–9750.
7 D. T. Chiu, E. Pezzoli, H. Wu, A. D. Stroock and G. M. Whitesides, *Proc. Natl. Acad. Sci. U. S. A.*, 2001, **98**, 2961–2966; M. J. Fuerstman, P. Deschatelets, R. Kane, A. Schwartz, P. J. A. Kenis, J. M. Deutch and G. M. Whitesides, *Langmuir*, 2003, **19**, 4714–4722; D. R. Reyes, M. M. Ghanem, G. M. Whitesides and A. Manz, *Lab Chip*, 2002, **2**, 113–116.
8 D. T. Eddington, R. H. Liu, J. S. Moore and D. J. Beebe, *Lab Chip*, 2001, **1**, 96–99.
9 A. K. Agarwal, L. Dong, D. J. Beebe and H. Jiang, *Lab Chip*, 2007, **7**, 310–315.
10 E. P. Kartalov, W. F. Anderson and A. Scherer, *J. Nanosci. Nanotechnol.*, 2006, **6**, 2265–2277.
11 K. Foster and G. A. Parker, *Fluidics: Components and Circuits*, Wiley-Interscience, New York, 1970; E. F. Humphrey, *Fluidics*, Fluidic Amplifier Associates, Boston, 1965.
12 T. Vestad, D. W. M. Marr and T. Munakata, *Appl. Phys. Lett.*, 2004, **84**, 5074–5075.
13 W. Zhan and M. Crooks Richard, *J. Am. Chem. Soc.*, 2003, **125**, 9934–9935.
14 W. H. Grover, R. H. C. Ivester, E. C. Jensen and R. A. Mathies, *Lab Chip*, 2006, **6**, 623–631.
15 J. Melin, N. Roxhed, G. Gimenez, P. Griss, W. van der Wijngaart and G. Stemme, *Sens. Actuators, B*, 2004, **B100**, 463–468.
16 M. L. Adams, M. L. Johnston, A. Scherer and S. R. Quake, *J. Micromech. Microeng.*, 2005, **15**, 1517–1521; L. F. Cheow, L. Yobas and D.-L. Kwong, *Appl. Phys. Lett.*, 2007, **90**(054107), 054101–054107; M. Prakash and N. Gershenfeld, *Science*, 2007, **315**, 832–835.
17 H. Zhang, X. Lin, Y. Yan and L. Wu, *Chem. Commun.*, 2006, 4575–4577; M. N. Stojanovic, T. E. Mitchell and D. Stefanovic, *J. Am. Chem. Soc.*, 2002, **124**, 3555–3561.
18 G. M. Walker and D. J. Beebe, *Lab Chip*, 2002, **2**, 131–134.
19 D. C. Duffy, J. C. McDonald, O. J. A. Schueller and G. M. Whitesides, *Anal. Chem.*, 1998, **70**, 4974–4984.
20 B.-H. Jo, L. M. Van Lerberghe, K. M. Motsegood and D. J. Beebe, *J. Microelectromech. Syst.*, 2000, **9**, 76–81.
21 Q. Yu, J. M. Bauer, J. S. Moore and D. J. Beebe, *Appl. Phys. Lett.*, 2001, **78**, 2589–2591; Q. Yu, J. S. Moore and D. J. Beebe, *Proc. μTAS*, 2002, **2**, 712–714.
22 D. J. Beebe, J. S. Moore, J. M. Bauer, Q. Yu, R. H. Liu, C. Devadoss and B.-H. Jo, *Nature*, 2000, **404**, 588–590; L. Dong, A. K. Agarwal, D. J. Beebe and H. Jiang, *Nature*, 2006, **442**, 551–554.